## Response to Referee #2

## November 20, 2025

We thank the reviewer for their additional comments. We have both provided a further analysis in our response here and updated the text in response to their concerns.

L160: "A new noise was generated" -> "A new noise value was randomly generated...". Just to clarify: did you use a Gaussian noise generator with standard deviation of NeDT?

• Yes, this is correct. The text has been updated to include the sentence: 'Each noise value was generated using a random Gaussian noise generator with standard deviation of  $0.75 \text{NE}\Delta\text{T}$ .'

L378: higher -> larger or coarser.

• Fixed.

Fig. 6d: is alarming. And I somewhat disagree with your explanation in Line 506-512. The consistent negative bias for integrated Dm is tied to those small IWC (the artifact in Fig. 6b for those samples with IWP  $< 1.\text{E-}2 \text{ kg/m}^2$ ) I believe.

• We are not certain if the reviewer meant to refer to lines 506-512, since these do not describe Fig. 6d. We therefore focus our response on the bias in the integrated retrieved  $D_{\rm m}$ , rather than the specific lines referred to.

We agree that the negative bias in Fig. 6d warrants an expanded discussion. We have expanded the text in the manuscript, but also respond in more detail here. The bias appears to arise due to several factors, the most influential being the overall tendency to underestimate  $D_{\rm m}^{IWC}$  across its full range, as seen in the retrieval performance figures in Fig. 8. While the mean and median in. Fig. 8 show only a small negative bias, the spread extends considerably lower, particularly at low altitudes and for low  $D_{\rm m}^{IWC}$ . As a result, these underestimations can substantially lower the integrated Dm values and contribute to the negative bias in Fig. 6d.

To illustrate this, we include an example for the reviewer's reference (Fig. 1). It is clear that the region of  $D_{\rm m}^{IWC}$  that contributes most to the integrated  $D_{\rm m}$  is highly underestimated in the retrieval. Interestingly, the low-magnitude artifacts mentioned by the reviewer are also visible in panel (d), but might actually act to reduce a negative bias.

We also find that such cases typically occur for low altitude clouds, which are more prone to underestimation at low  $D_{\rm m}^{IWC}$ . We isolated numerous cases of strong negative bias in the Dm integral, and all showed the same pattern — a localised underestimation of  $D_{\rm m}^{IWC}$  in the region contributing most to the integral. The cases of  $D_{\rm m}^{IWC}$  that are underestimated are not particularly high, and therefore contribute most strongly to the lower end of the distribution in Fig. 6d. These cases also tend to appear when IWP and IWC are relatively low.

For completeness, we also include the distribution of Dm column when all cases are included (Fig. 2), rather than filtering for IWP  $> 10^{-2}$  kg m<sup>-2</sup>, as done in Fig. 6d in the manuscript. In this case, the truth (integrated database) and retrieval (integrated retrieval) agree much more closely. This indicates that our model reproduces the overall training statistics well, and the filtering of the data unfortunately leads to a negative shift in the integrated Dm distribution. The difference between the integrated database and the database is due to the difference in

vertical resolution between the columns used to calculate each of these variables, as detailed in Sect. 4.3 of the manuscript.

Finally, there is also a negative bias present at the upper end of the  $D_{\rm m}$  range in Fig. 6d. We again attribute this to the underestimation of  $D_{\rm m}^{IWC} > 600~\mu{\rm m}$ , as shown in Fig. 8, which is consistent with the point at which the distributions begin to show stronger disagreement. This is a result also seen in May et al. (2024), when retrieving the column Dm directly.

## • The paragraph referring to Fig. 6d has now been updated in the manuscript, and is as follows:

'As done for IWP and  $Z_{\rm m}$  in Sect. 5.2, we also compare distributions of  $D_{\rm m}$ , which can be calculated from IWC and  $D_{\rm m}^{\rm IWC}$  according to Eriksson et al. (2020). Distributions are presented in panel (d) of Fig. 6. The distribution of direct retrievals of  $D_{\rm m}$  shows good agreement to the database-derived distribution. For  $D_{\rm m}$  calculated using retrieved  $D_{\rm m}^{\rm IWC}$ , the distribution agrees in shape with the database-derived distribution, but shows larger discrepancies than for  $Z_{\rm m}$ . Agreement is relatively good in the mid-range of  $D_{\rm m}$ . For  $D_{\rm m} < 100~\mu{\rm m}$  and  $D_{\rm m} > 700~\mu{\rm m}$ , poorer agreement is seen. This negative bias is attributed to a general underestino of  $D_{\rm m}^{\rm IWC}$  across most of its range. For example, cases of the integrated retrieved  $D_{\rm m} \sim 50~\mu{\rm m}$  were found to arise due to a strong underestimation of  $D_{\rm m}^{\rm IWC}$  at several altitudes in a profile, typically at low altitudes. These would be cases of relatively low  $D_{\rm m}^{\rm IWC}$  that lie close to or below the 16th quantile in Fig. 8, thus substantially lowering the column integral. Since  $D_{\rm m}^{\rm IWC} > 700~\mu{\rm m}$  is nearly always underestimated, the negative bias at high  $D_{\rm m}$  is likewise expected. Furthermore, unlike  $Z_{\rm m}$  which depends only on retrieved IWC,  $D_{\rm m}$  is derived from both retrieved IWC and retrieved  $D_{\rm m} \sim 50~\mu{\rm m}$  were also typically associated with low IWC, which are retrieved less accurately. Another plausible reason for the differences is that the IWC and  $D_{\rm m}^{\rm IWC}$  errors are correlated at each altitude. However, this information is not provided by QRNN.'

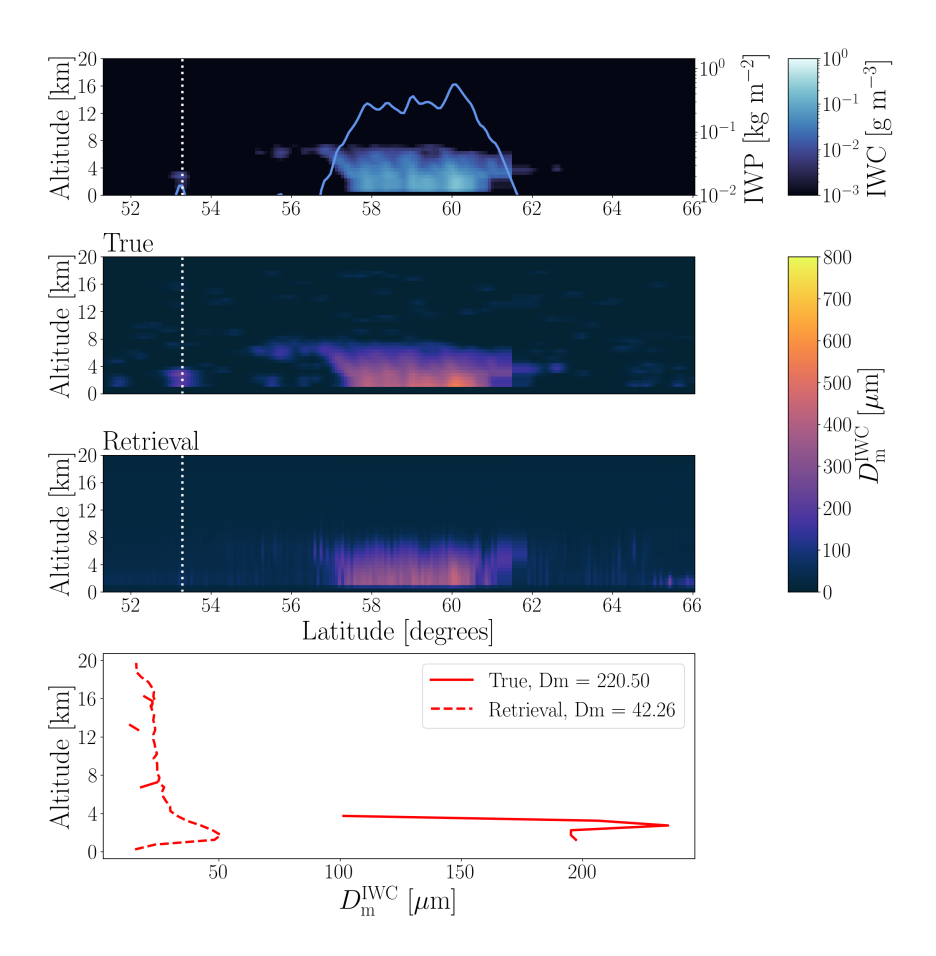


Figure 1: A scene of IWC,  $D_{\rm m}^{IWC}$ , and predicted  $D_{\rm m}^{IWC}$  is shown in panels a, b, and c, respectively. A specific case of integrated  $D_{\rm m}$  that has high negative bias is indicated in panels a, b and c by the dotted white line. The true and retrieved  $D_{\rm m}^{IWC}$  for this specific case is plotted in panel d, and the resulting integrated  $D_{\rm m}$  is given in the legend.

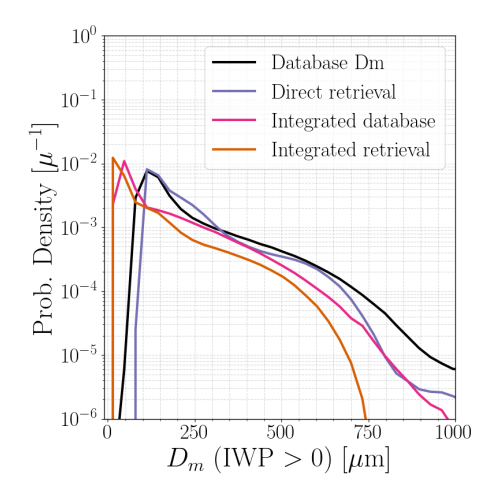


Figure 2: Distributions of  $D_{\rm m}$  calculated from database IWC and  $D_{\rm m}^{IWC}$ , calculated from retrieved IWC and  $D_{\rm m}^{IWC}$ , and a direct retrieval of Dm . The legend in panel (d) applies to both panel (c) and (d). Distributions of Zm and Dm are calculated only for cases corresponding to IWP  $> 10^{-2}$  kg m<sup>-2</sup>

L615: remove redundant "Fig.".

Fixed.

L798: The error covariance matrices also suggest the effective vertical resolution is  $\sim 2$  to 2.5 km, which is consistent with AK method derived value.

• The following sentence has been added to the 'Summary and conclusions' section: 'The retrieval error correlation matrices also suggest an effective vertical resolution of around 2 to 2.5 km, which is consistent with our estimations derived from averaging kernels.'

## References

Eriksson, P., Rydberg, B., Mattioli, V., Thoss, A., Accadia, C., Klein, U., and Buehler, S. A.: Towards an operational Ice Cloud Imager (ICI) retrieval product, Atmos. Meas. Tech., 13, 53–71, https://doi.org/10.5194/amt-13-53-2020, 2020.

May, E., Rydberg, B., Kaur, I., Mattioli, V., Hallborn, H., and Eriksson, P.: The Ice Cloud Imager: retrieval of frozen water column properties, Atmos. Meas. Tech., 17, 5957–5987, https://doi.org/10.5194/amt-17-5957-2024, 2024.